International Journal of Infrared and Millimeter Waves, Vol. 13, No. 4, 1992

MICROWAVE TRANSMISSION AND REFLECTION OF STRATIFIED LOSSY DIELECTRIC SEGMENTS PARTIALLY FILLING WAVEGUIDE

Xu Shanjia,[1] Wu Xinzhang,[1] P. Greiner,[2] C. R. Becker,[2] and R. Geick[2]

[1]*University of Science and Technology of China Hefei, Anhui, 230026, People's Republic of China*

[2]*Physikalisches Institut der Universität Am Hubland, 8700 Würzburg, Germany*

Received January 15, 1992

ABSTRACT

The microwave transmission and reflection is evaluated for stratified lossy dielectric segments partially filling the rectangular waveguide by the method which combines the multimode network theory with the rigorous mode matching procedure. As an example, we investigate in detail the microwave scattering properties of II-VI-epitaxial layer on a lossy dielectric substrate inserted in the rectangular waveguide. The experimental data verify the accuracy and the effectiveness of the present method. Extensive numerical results are presented to establish useful guidelines for the contactless microwave measurement of the conductivity of the epitaxial layer.

INTRODUCTION

The rectangular waveguide partially filled with dielectric and/or metallic materials has been studied for many years. Because of its practical applications such as phase shifters, impedance transformers,

0195-9271/92/0400-0569$06.50/0 © Plenum Publishing Corporation

polarization converters, mode transducers, harmonic separators, attenuators and various kinds of filters, a strong research interest in this guided wave structure has been documented in the literature.[1]-[3] When the losses of the dielectric and metallic materials are taken into account in the analysis and if the metal is considered to be a lossy dielectric with complex dielectric constant; all the above mentioned components can be united in a category of discontinuity consisting of the stratified lossy dielectric segments partially filling the rectangular waveguide. Therefore, the investigations of the scattering characteristics for this kind of discontinuity are of practical significance in microwave and millimeter wave engineering. Meanwhile, just as stated below, there is an important example that belongs to the same category of the complex dielectric discontinuity and promotes one to study this problem further.

As we know, II-VI-semiconductors have become more and more important in material science and engineering, because of their inherent advantages for applications in optoelectronic, infrared and millimeter wave techniques. For these purposes the exact knowledge of their electric properties, e.g. conductivity, are of essential significance. However, conducting II-VI-semiconductors have always created problems. In many cases, it is extremely difficult or even impossible to obtain good ohmic contacts to the sample. For characterising II-VI compounds under these circumstances, a contactless conductivity measurement [4] has been developped employing a microwave bridge technique. By this method, the conductivity of the semiconductor is obtained from the transmission coefficient of the sample which consists of the II-VI-epitaxial layer on a lossy dielectric substrate inserted in a rectangular waveguide. In this case the analysis of the scattering characteristics of the semiconductor sample is of undoubtedly practical significance.

In this paper, an accurate and simple method is presented to analyze the scattering characteristics, i.e. the transmission and reflection properties of stratified lossy dielectric segments inserted in the waveguide. As an example, we have determined theoretically the relationship between the conductivity of the semiconductor and the scattering parameters of the corresponding sample so that one can read the conductivity of the epitaxial layer from the measurement data of

the S-parameters directly. In such a way, the investigation of the semiconductor properties becomes more efficient and convenient. Since the present method combines the multimode network theory with the rigorous mode matching procedure and transfers the electromagnetic field boundary value problem into a network analysis problem, the whole calculation procedure is significantly simplified while still retaining the high accuracy of the mode matching method.

The validity of the present approach is justified by comparisons of the transmission coefficients for different samples between the experimental data and theoretical predictions. Extensive numerical results about the variations of the S-parameters with the sample parameters are given to establish useful guidelines for the contactless microwave measurement of the semiconductor sample.

METHOD OF ANALYSIS

Fig.1 shows the cross-sections of the stratified dielectric discontinuity structure under consideration. Here the dielectric constants of the epitaxial layer and the substrate are complex with large real and imaginary parts. for our semiconductor samples we assume the relative permeability $\mu = 1$, thus excluding semimagnetic samples. In the standard rectangular waveguide, the dominant mode is the TE_{10} mode, the fields of which are invariant in the y direction. Since the discontinuity is uniform in the same direction both in geometrical dimensions and in dielectric distributions, only TE_{m0} modes can be excited in the empty and in the partially filled waveguide. Therefore the scattering problem is two-dimensional. The solution procedure for this problem may be divided into two steps. First, we have to analyze the eigenvalue problem of the two waveguides, respectively, in the transverse cross-section. Secondly, we have to calculate the scattering characteristics of the discontinuity in the longitudinal cross-section. As the eigenvalues and the eigenfunctions for the empty waveguide are well known, the key point to the eigenvalue problem in the first step is the determination of the eigenvalues and the eigenfunctions in the partially filled waveguide. We have solved this problem with the microwave network method in which the electromagnetic boundary value problem is transfered to the impedance transformation in the

equivalent transmission line network, and the transverse resonance

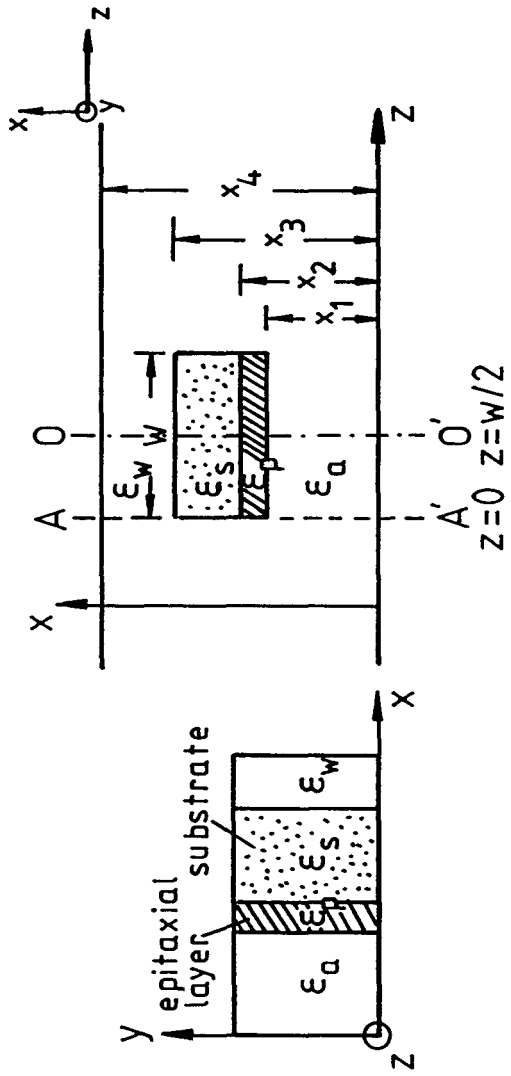

Fig.1 Cross-sections of the stratified lossy dielectric segment inserted in a rectangular waveguide.

technique is used to determine the eigenvalues and the eigenfunctions[5]. After solving the eigenvalue problem in the transverse cross-section of two waveguides, the second step is carried out with the method in which the mode matching procedure is treated as the transformation of the impedances inside and outside the discontinuity by introducing the coupling matrix taking into account the coupling of the modes in the two regions. Also the symmetry property of the structure in longitudinal direction is utilized to facilitate the calculation procedure[6]. The following considerations reveal the solution procedure in detail.

It is well known that the eigenfuctions and the eigenvalues of TE_{m0} modes for the empty rectangular waveguide are, respectively as follows, omitting phase factors like $\exp[j(\omega t - K_{zm}z)]$ here;

$$\phi_m = A_m sin(K_{xm}x) \tag{1}$$

$$K_{xm} = \frac{m\pi}{x_4} \tag{2}$$

$$K_{zm}^2 = K_0^2 - K_{xm}^2 \tag{3}$$

where K_0 is the free space wavenumber and the amplitude of the mth eigenmode A_m can be obtained with the orthonormal relation:

$$\int_0^{x_4} \phi_m^2 dx = 1.0 \tag{4}$$

$$A_m = \sqrt{\frac{2}{x_4}} \tag{5}$$

The transverse electromagnetic fields in the empty waveguide may be expressed in terms of the superposition of the complete set of the eigenmode functions as:

$$E_y = \sum_m^{\infty} V_m \phi_m \tag{6}$$

$$H_x = \sum_m^{\infty} I_m \phi_m \tag{7}$$

Just as mentioned before, the fields and the discontinuity structure are uniform in the y direction, we can move the two broad metallic surfaces of the waveguide filled with the sample to infinity without

changing the physics of the problem. As a result, the waveguide becomes a planar multilayer dielectric structure and its equivalent network representation is given in Fig.2. Because x=0 and x=x_4 planes are perfect conductors and the tangential field components at x=x_1, x_2 and x_3 must be continuous, the eigenfunctions of the partially filled waveguide can be presented as follows: [5] (all the quantities for the sample filled waveguide are indicated with top bar, and all phase factor with $(\omega t - \overline{K}_{zn} z)$ are again omitted)

$$\overline{\phi_n} = \begin{cases} \overline{A}_{4n} Sin\left[\overline{K}_{x4n}(x - x_4)\right] \\ \overline{A}_{3n} Sin\left[\overline{K}_{x3n}(x - x_3) - \Theta_{3n}\right] \\ \overline{A}_{2n} Sin\left[\overline{K}_{x2n}(x - x_2) - \Theta_{2n}\right] \\ \overline{A}_{1n} Sin\left(\overline{K}_{x1n} x\right) \end{cases} \tag{8}$$

where

$$\Theta_{2n} = j\left[\ln(-\Gamma_{2n})\right] / 2 \tag{9}$$

$$\Theta_{3n} = j\left[\ln(-\Gamma_{3n})\right] / 2 \tag{10}$$

$$\Gamma_{2n} = \left(\overline{\overline{Z}}_{2n} - \overline{Z}_{2n}\right) / \left(\overline{\overline{Z}}_{2n} + \overline{Z}_{2n}\right) \tag{11}$$

$$\Gamma_{3n} = \left(\overline{\overline{Z}}_{3n} - \overline{Z}_{3n}\right) / \left(\overline{\overline{Z}}_{3n} + \overline{Z}_{3n}\right) \tag{12}$$

$$\overline{Z}_{in} = \omega\mu / \overline{K}_{xin} \tag{13}$$

$$\overline{K}^2_{xin} = K_0^2 \varepsilon_i - \overline{K}^2_{zn} \tag{14}$$

$$i = 1, 2, 3, 4$$

$$\overline{K}^2_{zn} = K_0^2 \overline{\varepsilon}_{en} \tag{15}$$

$$\overline{\overline{Z}}_{3n} = j\,\overline{Z}_{4n} \tan\left(\overline{K}_{x4n} t_4\right) \tag{16}$$

$$\overline{\overline{Z}}_{2n} = \overline{Z}_{3n} \frac{\overline{\overline{Z}}_{3n} + j\,\overline{Z}_{3n} \tan\left(\overline{K}_{x3n} t_3\right)}{\overline{Z}_{3n} + j\,\overline{\overline{Z}}_{3n} \tan\left(\overline{K}_{x3n} t_3\right)} \tag{17}$$

The amplitudes $\overline{A}_{in}$ can be determined with the boundary conditions at each interface as follows:

$$\overline{A}_{2n} = -\overline{A}_{1n} Sin\left(\overline{K}_{x1n} t_1\right) / Sin\left(\overline{K}_{x2n} t_2 + \Theta_{2n}\right) \tag{18}$$

$$\overline{A}_{3n} = \overline{A}_{2n} Sin\Theta_{2n} / Sin\left(\overline{K}_{x3n} t_3 + \Theta_{3n}\right) \tag{19}$$

$$\overline{A}_{4n} = \overline{A}_{3n} Sin\Theta_{3n} / Sin\left(\overline{K}_{x4n} t_4\right) \tag{20}$$

Finally, the amplitude $\overline{A}_1$ then all the normalized amplitudes of the eigenfunctions can be obtained from the orthonormal relation:

$$\int_0^{x_4} \overline{\phi}_m^2 dx = 1 \tag{21}$$

Also, the transverse electromagnetic fields in the sample filled waveguide can be expressed in terms of the eigenfunctions as:

$$\overline{E}_y = \sum_n^{\infty} \overline{V}_n \overline{\phi}_n \tag{22}$$

$$\overline{H}_x = \sum_n^{\infty} \overline{I}_n \overline{\phi}_n \tag{23}$$

and the eigenvalues are calculated with the transverse resonance method as:

$$Z_{up} + Z_{dn} = 0 \tag{24}$$

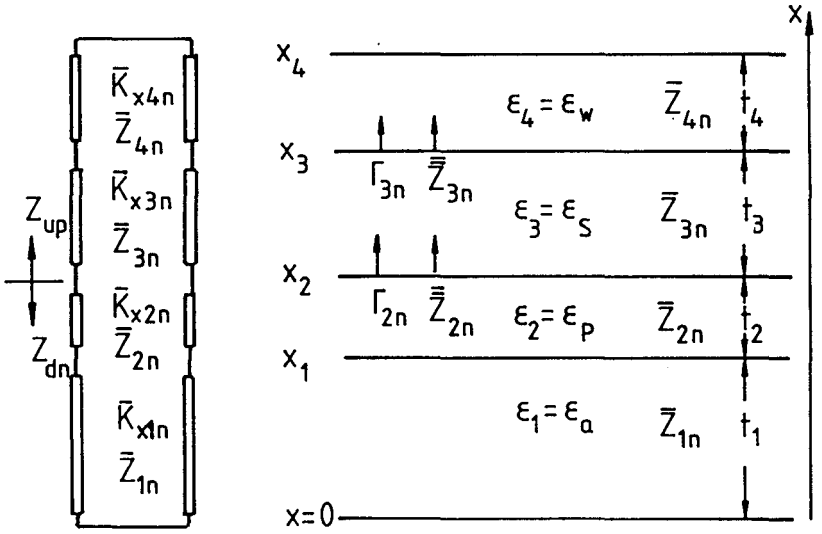

Fig.2 Planar multilayer dielectric structure and its equivalent network representation.

at any reference plane in principle. However, because the conductivity of the epitaxial layer is very large in the present case, it is better to choose the upper or the lower interface of the epitaxial layer as a reference plane to avoid missing modes.

At the discontinuity interface plane A-A' (z=0) the tangential fields E_y and H_x must be continuous, that is

$$E_y = \overline{E}_y \tag{25}$$
$$H_x = \overline{H}_x \tag{26}$$

or

$$\sum_m^{\infty} V_m \phi_m = \sum_n^{\infty} \overline{V}_n \overline{\phi}_n \tag{27}$$
$$\sum_m^{\infty} I_m \phi_m = \sum_n^{\infty} \overline{I}_n \overline{\phi}_n \tag{28}$$

these equations hold for any x in the z=0 plane. Scalar multiplying these equations with either $\overline{\phi}_n$ or ϕ_m and making use of the orthonormal relation:

$$\int_0^{x_4} \phi_i \phi_j dx = \delta_{ij} \tag{29}$$
$$\int_0^{x_4} \overline{\phi}_i \overline{\phi}_j dx = \delta_{ij} \tag{30}$$

we then have:

$$\mathcal{V} = \mathbf{Q}\overline{\mathcal{V}} \tag{31}$$
$$\mathcal{I} = \mathbf{Q}\overline{\mathcal{I}} \tag{32}$$

where $\mathcal{V}$, $\mathcal{I}$, $\overline{\mathcal{V}}$ and $\overline{\mathcal{I}}$ are column voltage and current vectors formed by the factors V_m, I_m, $\overline{V}_n$ and $\overline{I}_n$, respectively, representing the amplitudes of the electric field E_y and the magnetic field H_x outside and inside the discontinuity region. $\mathbf{Q}$ is the coupling matrix, its typical element Q_{ij} is

$$Q_{ij} = \int_0^{x_4} \phi_i \overline{\phi}_j dx \tag{33}$$

It can be proved that

$$QQ_t = Q_tQ = E \tag{34}$$

where 't' stands for transpose and E is the unit matrix. According to the definition of the impedance of multimode network, we have:

$$\mathcal{V} = Z\mathcal{I} \tag{35}$$
$$\overline{\mathcal{V}} = \overline{Z}\overline{\mathcal{I}} \tag{36}$$

and then we can obtain the relation

$$Z = Q\overline{Z}Q_t \tag{37}$$

where $\mathbf{Z}$ and $\overline{\mathbf{Z}}$ are, respectively, the input impedances on two sides of the discontinuity plane A-A' (z=0). This is actually a impedance transformation formula from which the reflection coefficient of each guided mode at z=0 plane can be determined.

It is worth to note that the present structure is symmetrical in longitudinal cross section as shown in Fig.3. The scattering of a guided mode by such a symmetrical structure may be analyzed in terms of the symmetrical and anti-symmetrical excitations for which we have the open-circuit (O.C.) and short-circuit (S.C.) bisections respectively, as indicated in Fig.3.

The reflection coefficient for each guided mode at the symmetry plane z=w/2 (O-O' plane) is 1.0 for the O.C. bisection or -1.0 for the S.C. bisection. Let $\mathbf{R}_0$ and $\mathbf{R}_s$ be the reflection coefficient matrices at z=0 plane for the O.C. and the S.C. bisections respectively; the guided mode reflection coefficient matrix $\mathbf{R}$ (at z=0 plane) and the transmission matrix $\mathbf{T}$ (at z=w plane) of the entire symmetrical structure are then given by:

$$R = (R_o + R_s) / 2 \tag{38}$$
$$T = (R_o - R_s) / 2 \tag{39}$$

For the dominant mode, the scattering parameters $S_{21} = S_{12}$ and $S_{11} = S_{22}$ are determined from the first row and the first column of $\mathbf{R}$ and

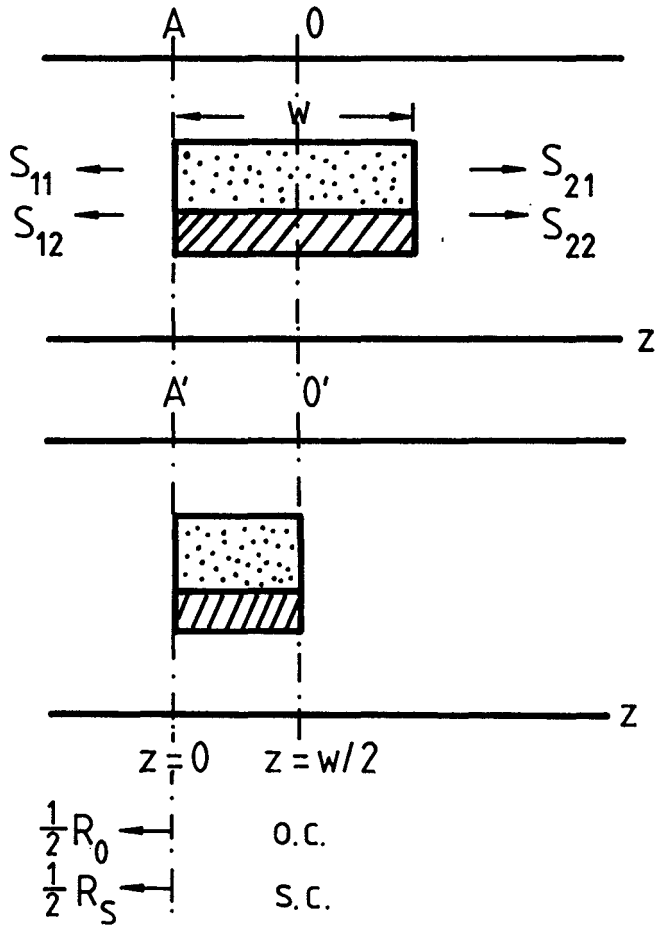

Fig.3 Symmetrical consideration of the structure in the longitudinal direction.

T matrices respectively as:

$$S_{11} = \boldsymbol{R}(1,1) = [\boldsymbol{R}_o(1,1) + \boldsymbol{R}_s(1,1)] \ / \ 2 \tag{40}$$

$$S_{21} = \boldsymbol{T}(1,1) = [\boldsymbol{R}_o(1,1) - \boldsymbol{R}_s(1,1)] \ / \ 2 \tag{41}$$

where matrices $\mathbf{R}_0$ and $\mathbf{R}_s$ are determined by:

$$\boldsymbol{R}_o = (\boldsymbol{Z}_o + \boldsymbol{Z}_c)^{-1} (\boldsymbol{Z}_o - \boldsymbol{Z}_c) \tag{42}$$

$$\boldsymbol{R}_s = (\boldsymbol{Z}_s + \boldsymbol{Z}_c)^{-1} (\boldsymbol{Z}_s - \boldsymbol{Z}_c) \tag{43}$$

with

$$Z_o = Q\overline{Z}_o Q_t \quad (44)$$

$$Z_s = Q\overline{Z}_s Q_t \quad (45)$$

the matrices $\mathbf{Z}_0$, $\mathbf{Z}_s$, $\mathbf{Z}_c$ are all of diagonal form their typical elements are respectively, given as follows:

$$\overline{Z}_{0n} = -j\,\overline{Z}_n \cot\left(\overline{K}_{zn} w/2\right) \text{ for O} - \text{O}' \text{ plane being O.C.} \quad (46)$$

$$\overline{Z}_{sn} = j\,\overline{Z}_n \tan\left(\overline{K}_{zn} w/2\right) \text{ for O} - \text{O}' \text{ plane being S.C.} \quad (47)$$

$$\overline{Z}_n = \omega\mu/\overline{K}_{zn} \quad (48)$$

$$Z_{cm} = \omega\mu/K_{zm} \quad (49)$$

NUMERICAL RESULTS

Table 1 presents a comparison of the transmission characteristics for different samples between the experimental data and the theoretical predictions. It can be seen from the table that the agreement is very good for the transmission coefficient $S_{21} =\mid S_{21} \mid \exp(j\varphi_{21})$. The reliability and the accuracy of the present method are thus justified.

Table 1. Comparison of the transmission coefficients for different samples between the experimental data and the theoretical predictions

sample σ (mhos/cm)		$\lvert S_{21}\rvert$ (dB)		φ_{21} (degree)	
		test	theory	test	theory
CMT78	($\sigma = 9.0$)	-3.25	-3.33	-63.2	-63.75
CMT76	($\sigma = 38.5$)	-5.30	-5.19	-56.2	-55.77
Q154	($\sigma = 67.0$)	-8.90	-9.44	-28.2	-27.41
Q114	($\sigma = 510.0$)	-10.65	-10.28	31.7	39.22
Q107	($\sigma = 1107.0$)	-10.50	-10.47	36.8	38.74
Q105	($\sigma = 1470.0$)	-10.90	-10.32	31.8	38.32

The dispersion relation (24), the impedance transformation formula (37) and the guided mode reflection and transmission coefficient formulae (38) and (39) are exact in principle, but the procedure involves matrices of infinite dimensions which have to be truncated for a numerical analysis. Therefore, the convergence property of the solution is one of the most important factors in evaluating an analysis method. Table 2 presents the convergence properties of the calculations with the increasing truncation number, i.e. the number of modes used, for different samples. It turns out that the convergence is quite good; all the calculation values converge to their own asymptotic values steadily within relatively small mode numbers. With respect to the attenuation only 9 to 11 modes are good enough for lower conductivity. Even for higher conductivity, 25 modes are enough to get the accurate results. With respect to the phases, higher mode numbers are necessary to obtain the final values; they are 13 to 15 modes for lower conductivity and more than 27 modes for higher conductivity.

Table 2. Convergence properties of the calculations with increasing mode number for different samples

mode number	CMT78		CMT76		CMT70*	
	$\lvert S_{21}\rvert$	φ_{21}	$\lvert S_{21}\rvert$	φ_{21}	$\lvert S_{21}\rvert$	φ_{21}
1	-3.80	-64.17	-5.69	-53.77	-9.20	41.96
3	-3.46	-64.07	-5.35	-55.27	-9.54	40.30
5	-3.38	-63.91	-5.25	-55.60	-9.85	40.39
7	-3.35	-63.83	-5.21	-55.67	-9.99	40.44
9	-3.33	-63.80	-5.20	-55.73	-10.07	40.45
11	-3.33	-63.78	-5.19	-55.75	-10.11	40.44
13	-3.33	-63.76	-5.19	-55.76	-10.15	40.45
15	-3.33	-63.75	-5.19	-55.77	-10.18	40.43
17	-3.33	-63.75	-5.19	-55.77	-10.20	40.41
19	-3.33	-63.75	-5.19	-55.77	-10.22	40.38
21	-3.33	-63.75	-5.19	-55.77	-10.23	40.36
23	-3.33	-63.75	-5.19	-55.77	-10.25	40.35
25	-3.33	-63.75	-5.19	-55.77	-10.27	40.24
27	-3.33	-63.75	-5.19	-55.77	-10.27	40.23
29	-3.33	-63.75	-5.19	-55.77	-10.27	40.23

$* \sigma = 1620.0\ (mhos/cm)$

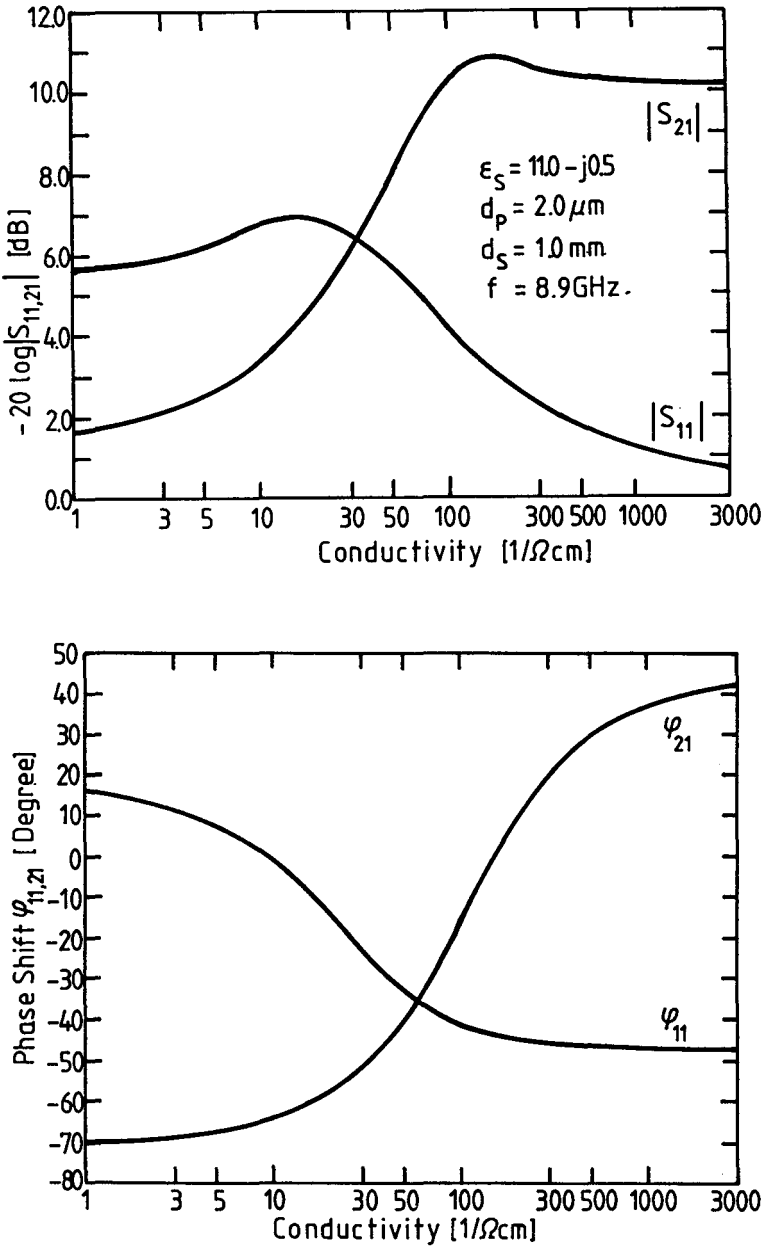

Fig.4 Parameters S_{11} and S_{21} versus conductivity of the epitaxial layer.

Fig.4 shows the parameters S_{21} and $S_{11} = | S_{11} | \exp(j\varphi_{11})$ versus the conductivities of the epitaxial layer. The variations of the curves are as expected, because the conductivity of the epitaxial layer has a strong influence on the field distributions in the waveguide. For instance, when the conductivity is small, say less than 15.0 (mhos/cm), the dominant mode in the sample filled waveguide is a propagating mode. In this region therefore, $| S_{21} |$ keeps flat in its maximum and

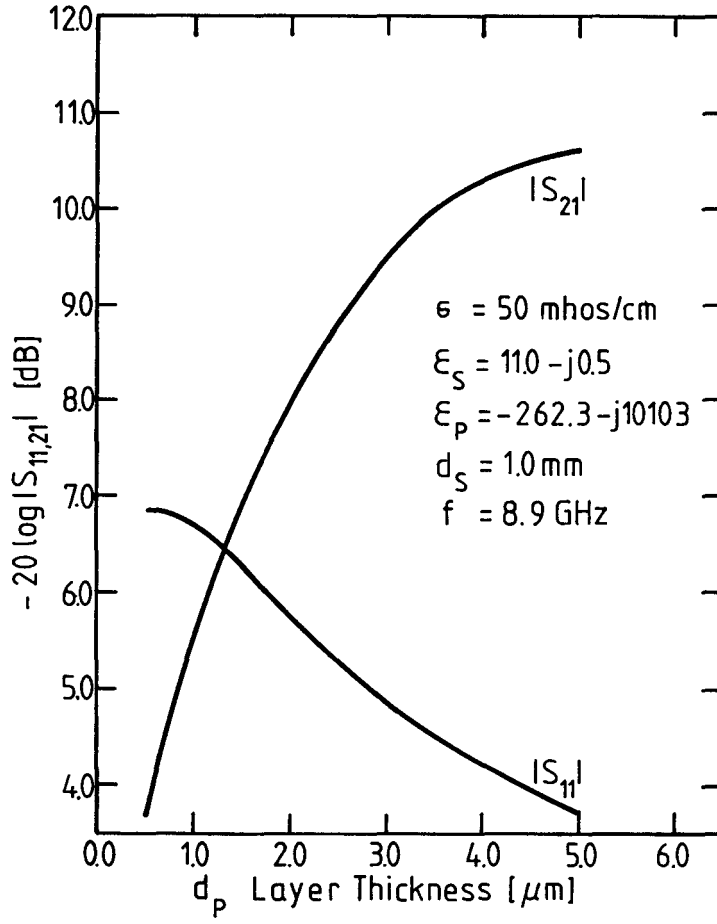

Fig.5(a) Variations of $|S_{11}|$,$|S_{21}|$ with thickness of epitaxial layer.

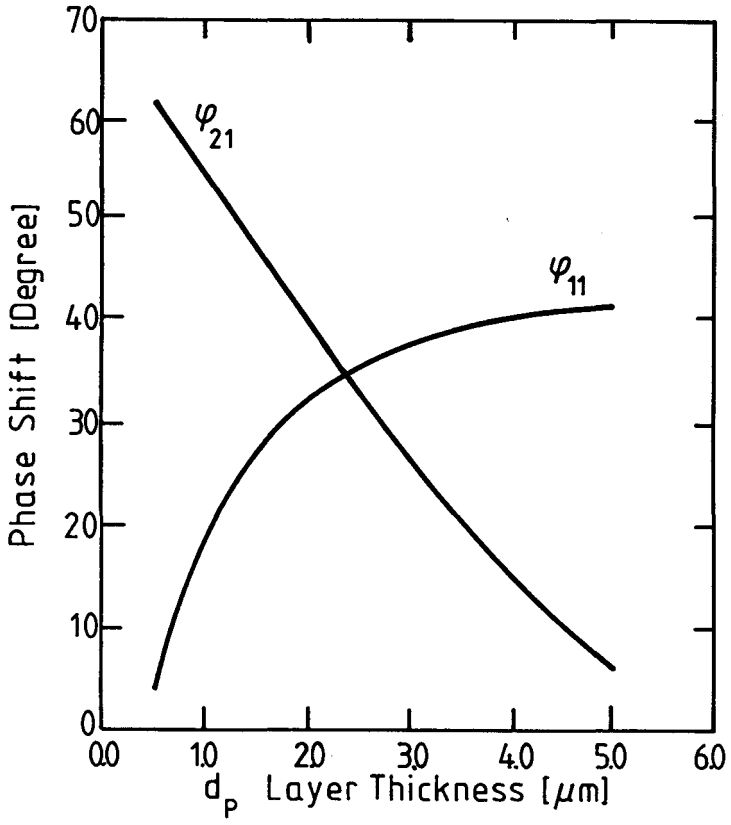

Fig.5(b) Variations of φ_{11}, φ_{21} with thickness of epitaxial layer.

reduces gradually as σ increases. When σ increases beyond a critical value, the dominant mode suddenly becomes a cutoff mode; this makes $|S_{21}|$ decrease rapidly with σ increasing. As σ is further increased the dominant mode falls below cutoff deeper and deeper and finally the electromagnetic fields of the dominant mode approach the complete standing wave distribution in the transverse cross-section which just corresponds to the case that a perfect conductor is placed at the position where the epitaxial layer is located. In this case, $|S_{21}|$ reaches its minimum and is little affected as σ increases. From the curves, it is seen that the amplitude and the phase of the transmission coefficient

and the reflection coefficient vary with conductivity of the layer in a different way; $|S_{21}|$ and φ_{11} are insensitive in high conductivity region whereas $|S_{11}|$ and φ_{21} change rapidly in the same region. Based on these characteristics, it may be suggested that it is better to measure $|S_{11}|$ or φ_{21} for the epitaxial layer with high conductivity; on the contrary, it is recommended to measure $|S_{21}|$ or φ_{11} for the epitaxial layer with low conductivity.

Fig.5 gives the variation of the S-parameters with the thickness of the epitaxial layer. It can be seen from the figure that $|S_{21}|$ has its maximum and $|S_{11}|$ keeps in its minimum for $d_p \simeq 0$ because in this case the loss of the sample originates mainly from the dielectric substrate, and the loss of the substrate is relatively small compared with that of the epitaxial layer. Since the real part of the dielectric constant of the substrate is quite large, the electromagnetic fields concentrate in the substrate region and decay exponentially along the x direction in the air region. The increase of the thickness d_p can be considered as adding more loss material to the structure. When the thickness is increased from zero, but not to much, say $0.0 < d_p < 4.0$ (μm), the loss material is in a region with strong fields; its effect on $|S_{21}|$ decreases and $|S_{11}|$ increases rapidly with increasing thickness. However, when the thickness d_p is further increased, the additional loss material appears in a region where the fields are exponentially small, and have little effect on the S-parameters.

Fig. 6 presents the variation of the S-parameters with the substrate thickness d_s. The curves show that the effect of d_s on the amplitude of $|S_{21}|$ and $|S_{11}|$ are not so strong, because the losses of whole structure originate mainly from the epitaxial layer. With increasing d_s, $|S_{21}|$ is nearly constant and $|S_{11}|$ increases slightly.

Fig. 7 shows the variation of the S-parameters with measurement frequencies. Since the changes of the dielectric constants for both substrate and epitaxial layer are not so large as frequency is increased, the effect of frequency on the amplitude of $|S_{21}|$ and $|S_{11}|$ are not so strong. All these numerical results are helpful to establish useful guidelines for the contactless microwave measurement of the conductivity of the epitaxial layer.

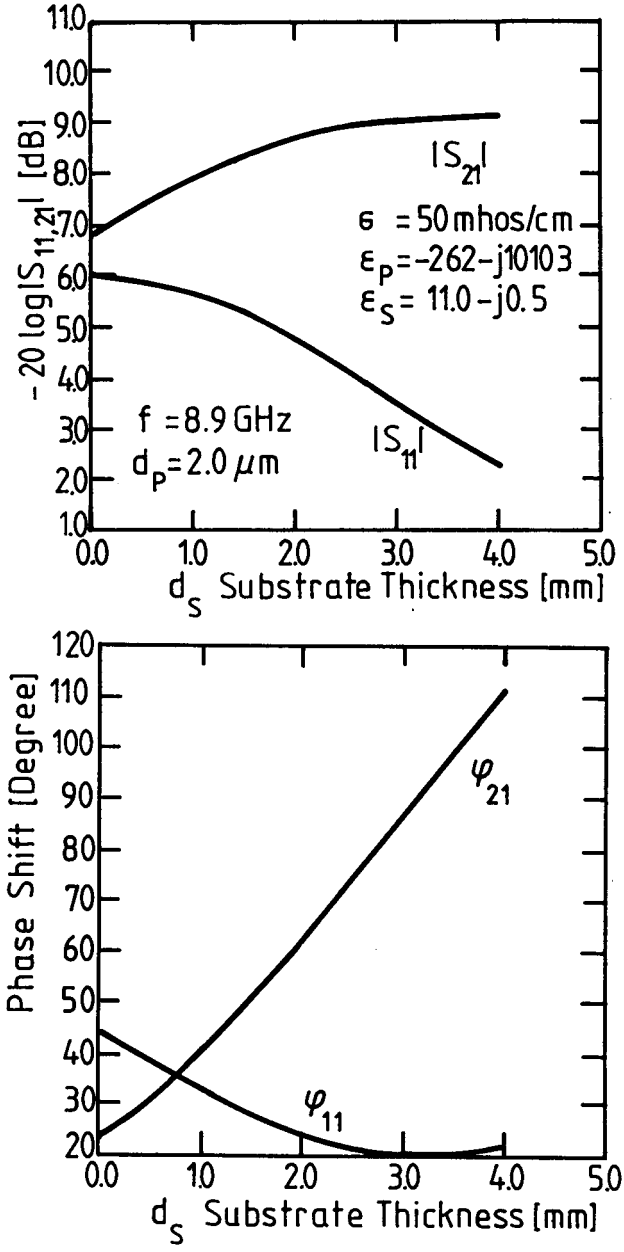

Fig.6 Variations of S_{11} and S_{21} with substrate thickness.

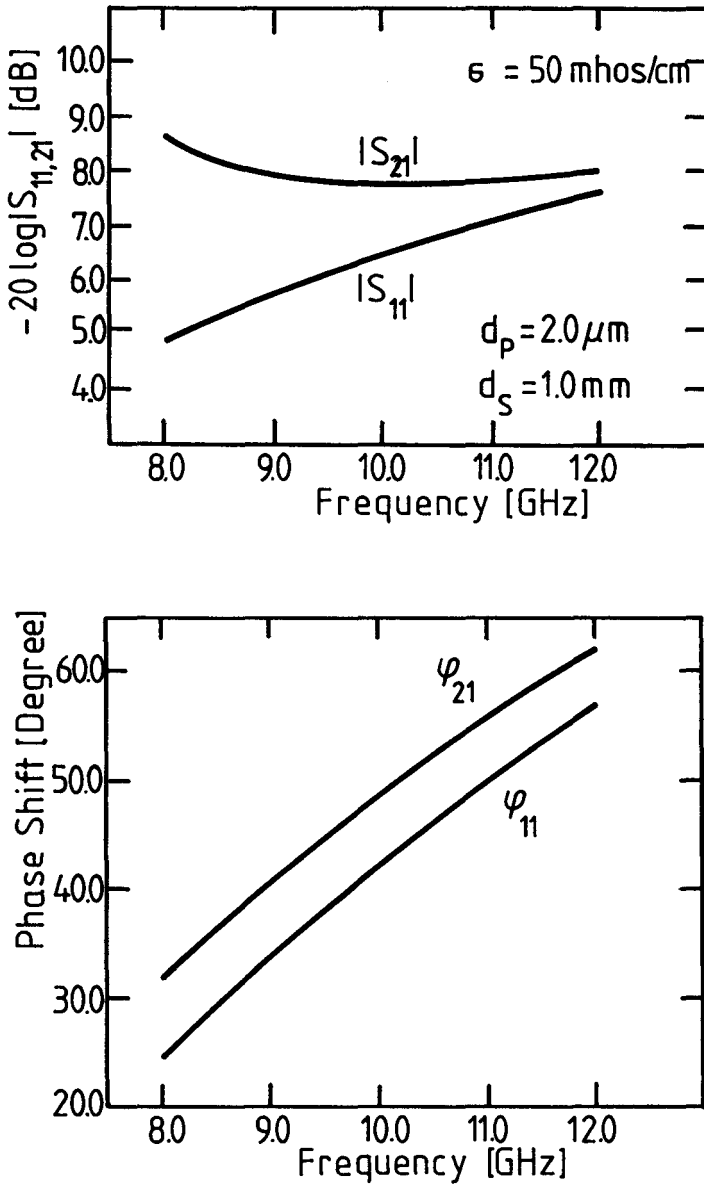

Fig.7 Variations of S_{11} and S_{21} with measurement frequencies.

ACKNOWLEDGEMENTS

This work was supported by The National Natural Science Foundation of China and The Deutsche Forschungsgemeinschaft.

REFERENCES

[1] C.T.Liu, IEEE Trans. on MTT Vol.27, No.8, 1981,pp.805-810.

[2] Xu Shanjia, Journal of Electronics, Vol.6, No.3, 1989, pp. 232-241.

[3] Y. Konish, IEEE Trans. on MTT Vol.22, No.10, 1974, pp.869-873.

[4] P. Greiner, L.Polignone, C.R. Becker, R. Geick, Digest of 16th IC on IR and MMW, 1991, pp.308-309.

[5] Xu Shanjia, Journal of Electronics, Vol.6, No.1, 1989,pp.50-58.

[6] Xu Shanjia, S. T. Peng and F. K. Schwering, IEEE Trans. on MTT Vol.37, No.4, 1989, pp.686-690.